United States Patent

Denison et al.

[15] **3,648,046**

[45] **Mar. 7, 1972**

[54] QUADRUPOLE GAS ANALYZER COMPRISING FOUR FLAT PLATE ELECTRODES

[72] Inventors: **Dean R. Denison; Charles F. Morrison, Jr.,** both of Boulder, Colo.

[73] Assignee: **Granville-Phillips Company,** Boulder, Colo.

[22] Filed: **May 18, 1970**

[21] Appl. No.: **38,076**

[52] **U.S. Cl.**.....**250/41.9 DS,** 250/41.9 G, H01j/39/34

[51] **Int. Cl.**.....**B01d 59/44**

[58] **Field of Search**.....250/41.9 DS

[56] **References Cited**

UNITED STATES PATENTS

2,950,389	8/1960	Paul	250/41.9 DS
3,501,631	3/1970	Arnold	250/41.9 DS

Primary Examiner—Walter Stolwein
Assistant Examiner—C. E. Church
Attorney—Gerald J. Ferguson, Jr.

[57] **ABSTRACT**

A quadrupole analyzer wherein the trajectory stability of the charged particles is determined by two parameters a and q where

$$a = \frac{eU}{Kmw^2r_0^2}$$

and

$$q = \frac{eV}{2Kmw^2r_0^2}$$

where

K = any value except $0.125 \leq K \leq 0.126$.

A further aspect of the invention relates to performance optimization of a quadrupole analyzer in the presence of relatively large amplitude, nonquadrupole field components.

15 Claims, 16 Drawing Figures

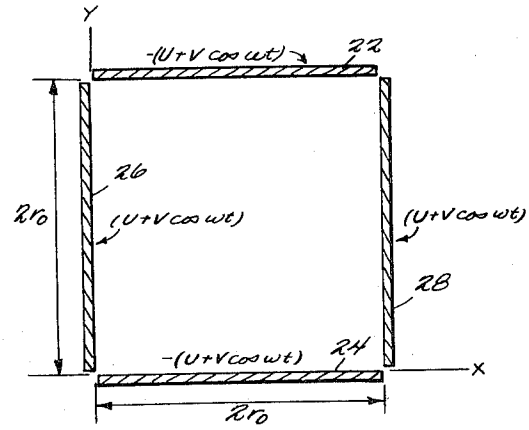
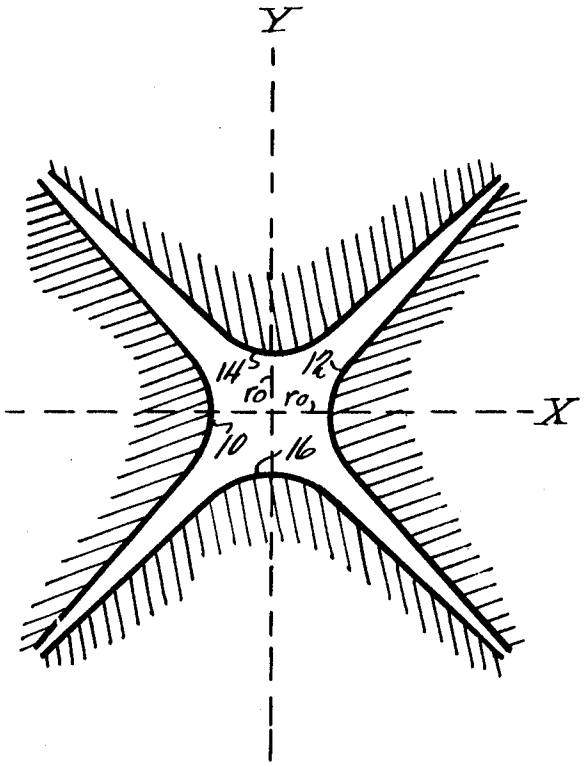


Fig. 1
(PRIOR ART)



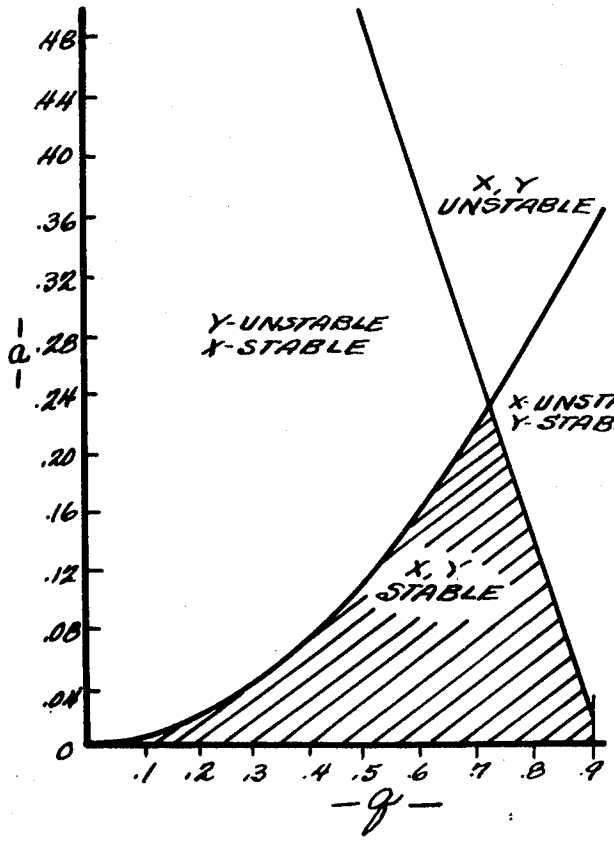


Fig. 2

INVENTORS
DEAN E. DENISON
CHARLES F. MORRISON, JR.

BY Gerald J. Ferguson Jr.
ATTORNEY

FIG. 3

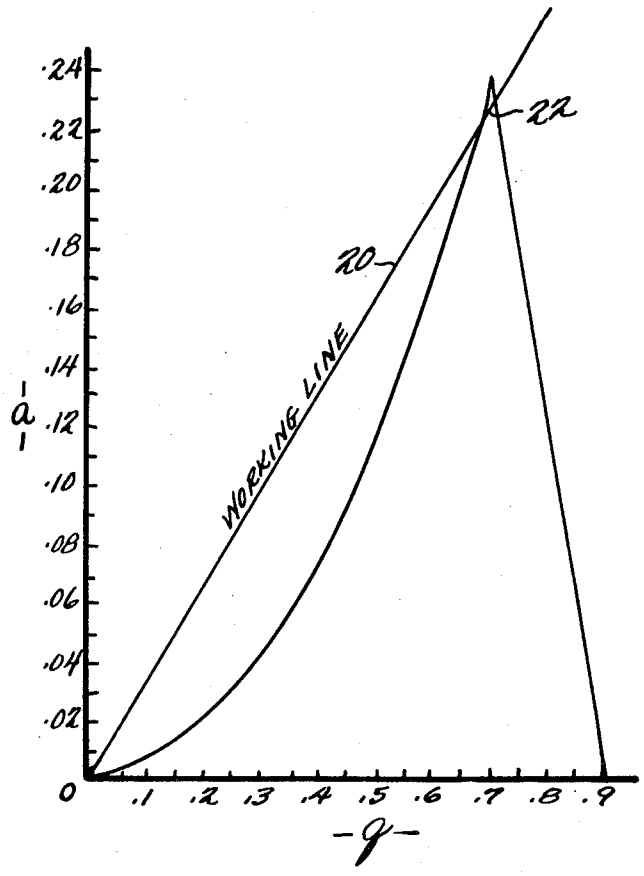
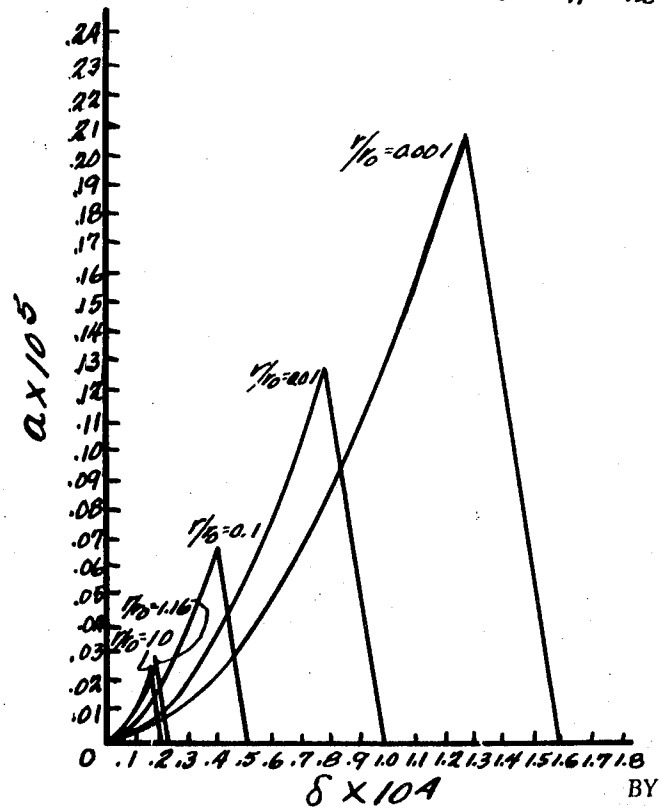


FIG. 4



INVENTORS
DEAN R. DENISON
CHARLES F. MORRISON, JR.

BY Gerald J. Ferguson Jr.
ATTORNEY

Fig. 5

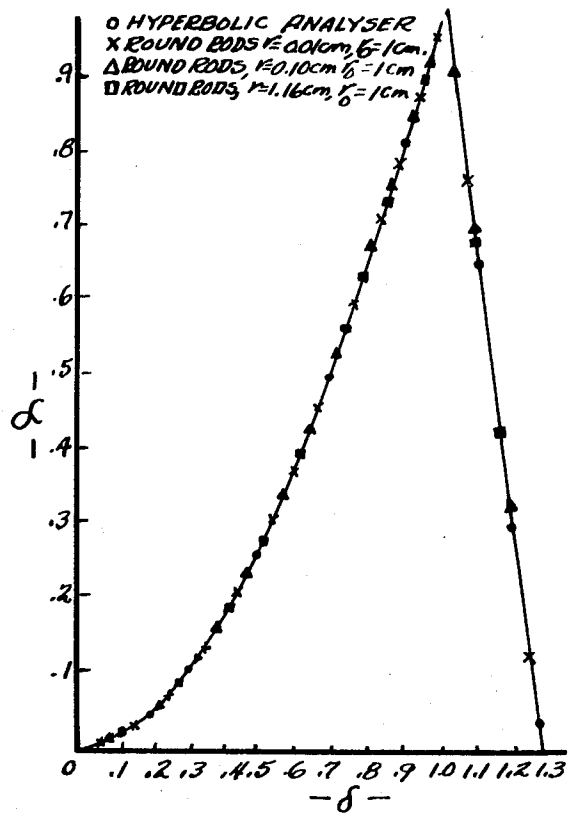
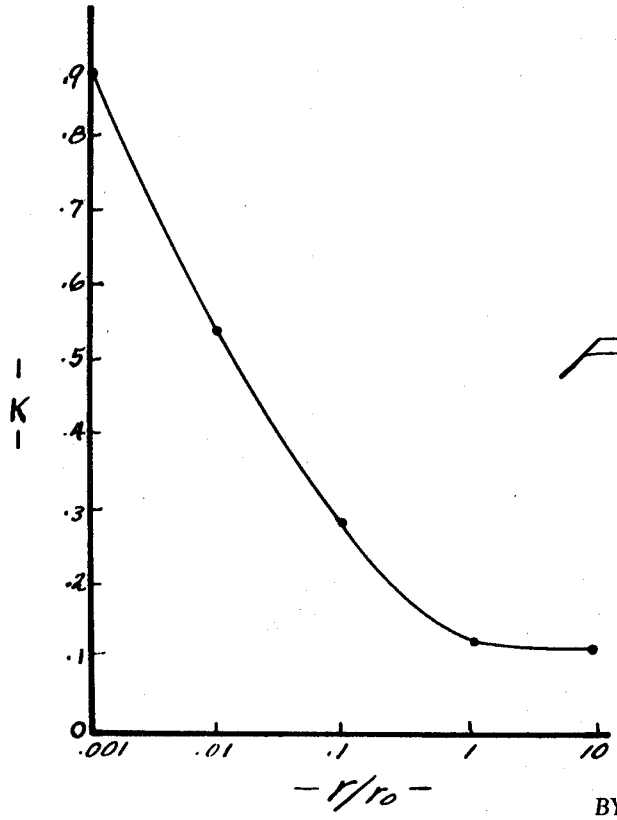


Fig. 6



INVENTORS
DEAN R. DENISON
CHARLES F. MORRISON, JR.

BY Gerald J. Ferguson Jr.
ATTORNEY

Fig. 7

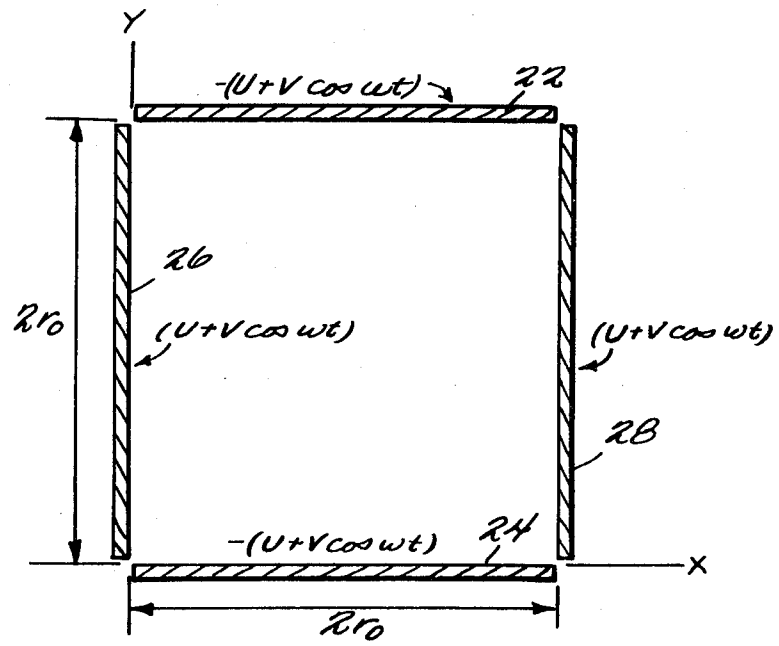
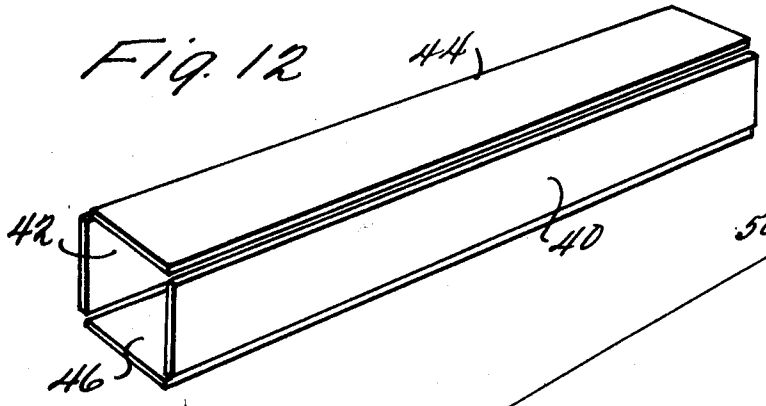


Fig. 12



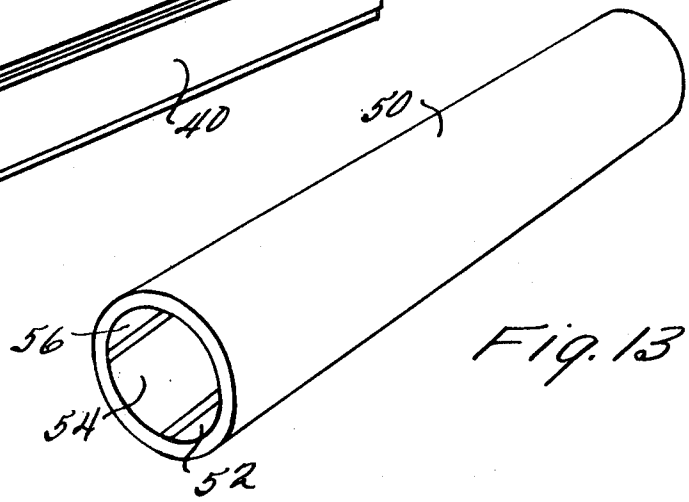


Fig. 13

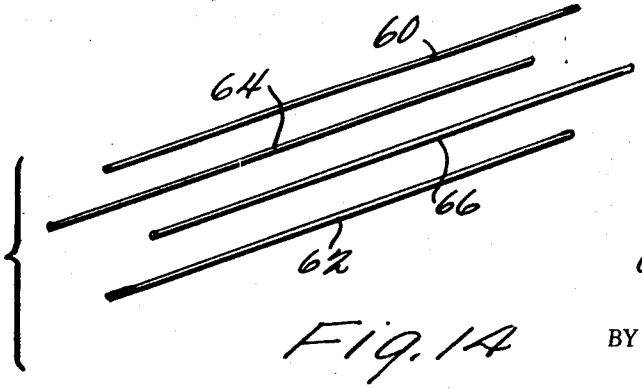
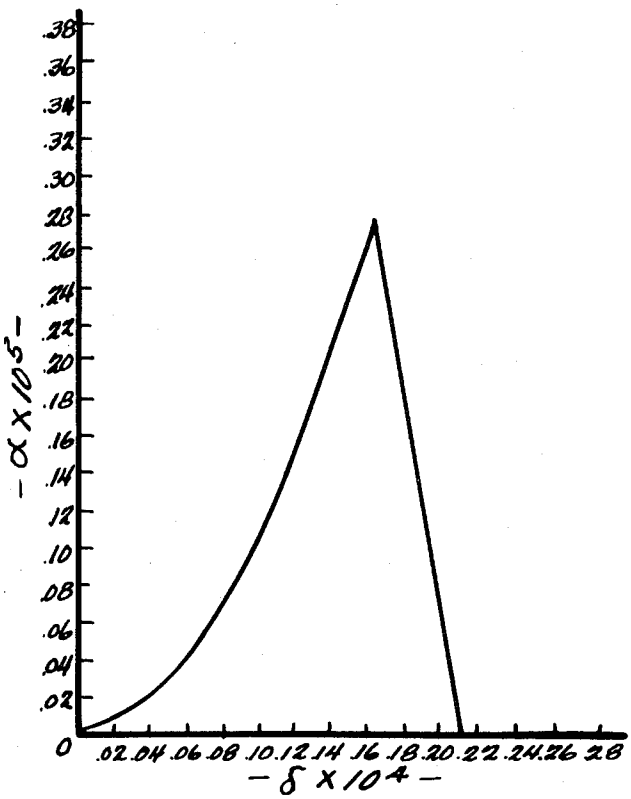


Fig. 14

INVENTOR
DEAN R. DENISON
CHARLES F. MORRISON, JR.

BY Gerald J. Ferguson Jr.
ATTORNEY

Fig. 8



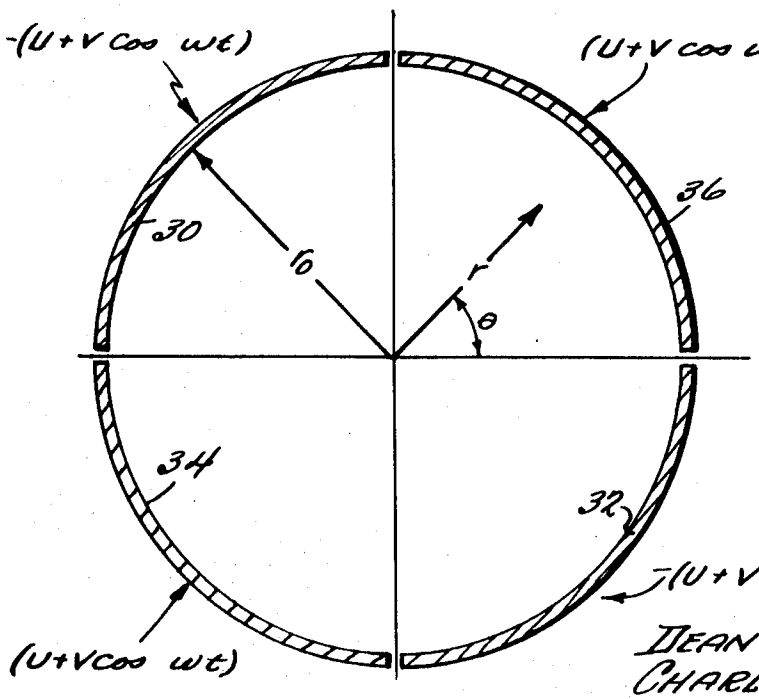
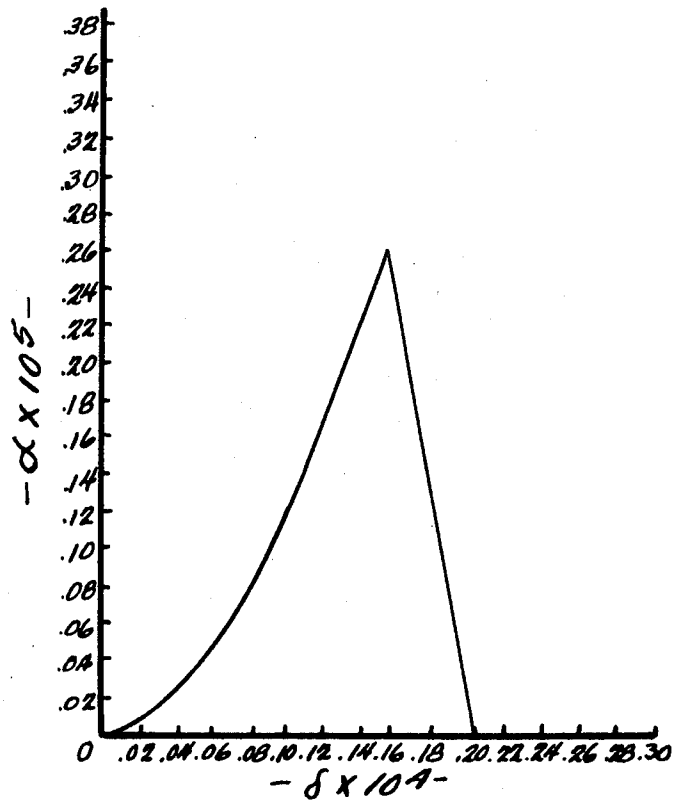


Fig. 9

INVENTORS
DEAN R. DENISON
CHARLES F. MORRISON, JR.

BY Gerald J. Ferguson Jr.
ATTORNEY

Fig. 10



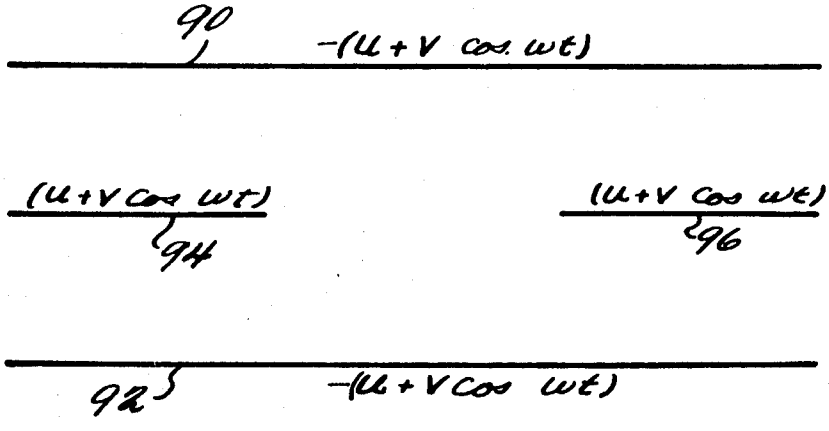
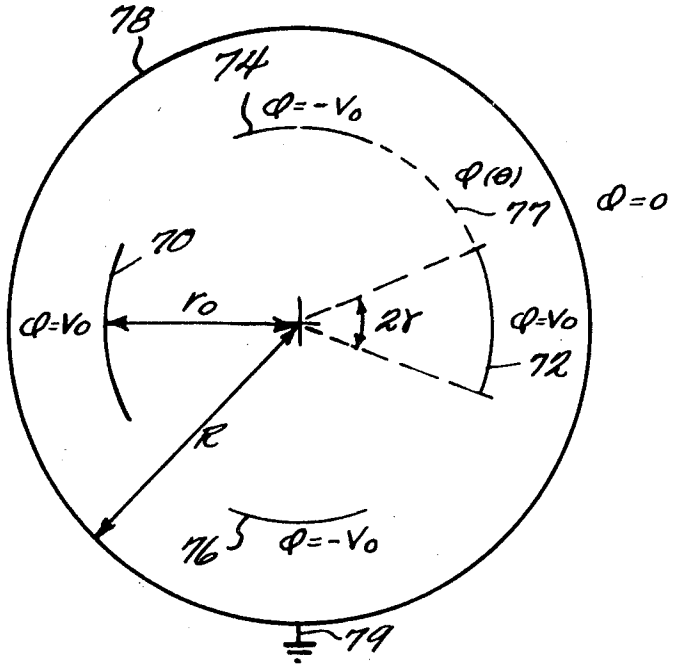


Fig. 11

INVENTORS
DEAN R. DENISON
CHARLES F. MORRISON, JR.

BY Gerald J. Ferguson Jr.
ATTORNEY

Fig. 15



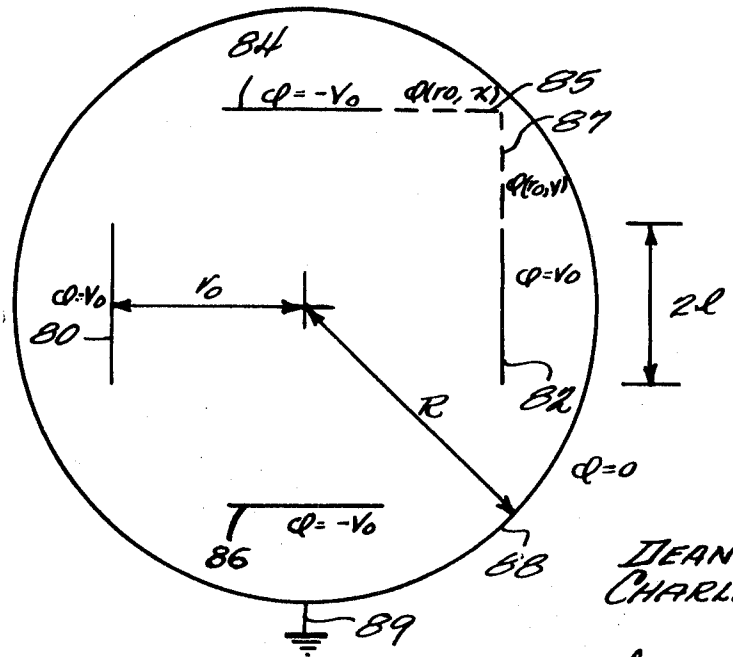


Fig. 16

INVENTOR
DEAN R. DENISON
CHARLES F. MORRISON, JR.

BY Gerald J. Ferguson Jr.
ATTORNEY

QUADRUPOLE GAS ANALYZER COMPRISING FOUR FLAT PLATE ELECTRODES

BACKGROUND OF THE INVENTION

This invention relates to an improved quadrupole-type gas analyzer for separating charged particles, usually positive or negative ions, by utilizing electric fields to separate said charged particles by their charge to mass ratio.

In 1953, Paul and Steinwedel introduced the concept of using a time varying quadrupole field as a mass separator and in 1955, Paul and Raether demonstrated that a practical device could be produced to separate ions of differing mass.

The theory of Paul and Steinwedel assumes that the electrode structure required to generate the quadrupole field consists of hyperbolic cylinders or electrodes **10–16** (see FIG. **1**) with semiaxes both equal to a distance r_o, the so-called field radius. The hyperbolic cylinders **10–16** are connected to alternating and direct current sources such that the two electrodes **10** and **12** on the X axis receive a voltage $(U+V\cos w\,t)$ where U is the DC voltage, V is the half-amplitude of the AC voltage, w is the angular frequency of the AC voltage, and t is time and the two electrodes on the y axis receive a voltage $-(U+V\cos w\,t)$. Thus, the DC polarity of the y axis electrodes is reversed from the X axis electrodes and the two sets of electrodes have AC voltages 180° out of phase from each other.

Although an admitted oversimplification, the mass separation can be visualized in the following way. With some set of AC and DC voltages on the electrodes, ions with masses that are lighter than some value will be strongly influenced by the AC voltage and will remain in phase with that voltage. Thus, energy will be taken from the field and the amplitude of the motion of such a particle will increase until it is captured on an electrode. An ion with mass heavier than some value will not be affected appreciably by the AC field and will be dragged to one of the y axis electrodes by the DC field. It then follows that there is some mass such that the AC and DC fields tend to balance each other and such a mass will follow a stable trajectory through the analyzer. More theoretically, the equation of motion of an ion through the combined AC–DC field can be expressed as a linear sum of Mathieu functions where the ion trajectory stability is determined by two parameters, a and q, defined by

$$a=\frac{8eU}{mw^2r_0^2}, \qquad q=\frac{4eV}{mw^2r_0^2}$$

where m is the ionic mass and e is the charge. a and q are related in a complex way. Graphically, a and q can be plotted as in FIG. **2** and the stability criteria intuitively described above can be determined. The shaded region contains those values of a and q (this is actually only one of many stability regions—but the most useful in a practical device) for which an ion executes a stable trajectory through the analyzer. For a constant ratio of DC and AC voltages, the ratio of a to q is a constant and is graphically represented by the straight line, commonly referred to as the "working line," as shown at **20** in FIG. **3**. For an analyzer with a given value of r_o and operating at some frequency w, it can be seen from the definitions of a and q that the ionic masses can be considered to be spread out along the working line with the heavier masses nearer the origin. As the voltages are scanned from zero to some maximum value, with the ratio of a to q, and hence DC to AC voltage ratio, held constant, the masses slide along the working line with only those masses falling within the stability region executing stable trajectories. Thus, as the voltage is scanned from zero to some value a plot of the ion current passing through the analyzer as a function of the voltage a mass spectrum is generated. The working line as shown in FIG. **3** intersects the stability region such that some range of masses execute stable trajectories, as indicated at **22**. As the slope, and hence the ratio of a to q, is increased the range becomes narrower until intersection of the working line with the stability diagram occurs at only one point and hence only a single mass executes a stable trajectory. Thus, as the slope of the working line is increased, the resolution increases. Obviously if the slope of the working line is increased further, no ions execute stable trajectories. This, then, is briefly how the analyzer functions.

In actual practice, the difficulty and expense of producing precision hyperbolic electrodes has forced the expedient of approximating the hyperbolic surfaces with cylindrical surfaces. In the literature, the teaching has been that the most satisfactory substitution is a round rod with a radius of $1.15\,r_o$ in analogy to a field study of a magnetic quadrupole made by I. E. Dayton. Further, the teaching of the literature claims that such substitution of round rods of radius $1.15\,r_o$ for the hyperbolic surfaces is an expedient only, and that degradation of performance results.

However, it has been determined by the inventors that the above teaching is not true and that unexpectedly improved results are obtained by deviating from that teaching.

DETAILED DESCRIPTION OF THE DRAWING

FIG. **1** is a cross-sectional illustration of a prior art quadrupole analyzer.

FIG. **2** is a graph illustrating one of the stability regions of the analyzer of FIG. **1**.

FIG. **3** is a graph illustrating the operation of the analyzer of FIG. **1**.

FIG. **4** is a graph which illustrates stability regions or diagrams obtained for a number of round rod diameters.

FIG. **5** is a graph which illustrates the diagrams of FIGS. **4**, **8**, and **10** when normalized.

FIG. **6** is a graph illustrating K as a function of round rod radius for round rod analyzers.

FIG. **7** is a cross-sectional illustration of a flat plate analyzer in accordance with this invention.

FIG. **8** is a graph which illustrates a stability region or diagram associated with the analyzer of FIG. **7**.

FIG. **9** is a cross-sectional illustration of a circular concave analyzer.

FIG. **10** is a graph which illustrates a stability region or diagram associated with the analyzer of FIG. **9**.

FIG. **11** is a cross-sectional illustration of a modified quadrupole in accordance with the invention.

FIG. **12** is a diagrammatic illustration of one embodiment of the flat plate analyzer of FIG. **7**.

FIG. **13** is a diagrammatic illustration of one embodiment of the circular concave analyzer of FIG. **9**.

FIG. **14** is a diagrammatic illustration of one embodiment of a small wire analyzer in accordance with the invention.

FIG. **15** is a diagrammatic illustration of a circular concave analyzer together with an enclosure therefor in accordance with a further aspect of the invention.

FIG. **16** is a diagrammatic illustration of a flat plate analyzer together with an enclosure therefor in accordance with a further aspect of the invention.

DETAILED DESCRIPTION OF PREFERRED EMBODIMENTS OF THE INVENTION

Theoretical analysis of the potential distributions of various electrode arrangements have been made and stability diagrams similar to FIG. **2** have been established. Each of the arrangements which were analyzed will now be discussed. Generalized conclusions will then be stated.

Round Rod Analyzer

An analytic expression for the potential in the vicinity of round rods, with potentials as described for FIG. **1**, is not readily obtained. However, the potential distribution was obtained numerically by constructing a grid and computing a solution to Laplace equation using the Liebmann process. Once the potential distribution is known, the x and y potential gradients are obtainable and thus the forces on an ion at any point within the rod structure are known. A computer is then employed to "follow" an ion through the rod structure and

determine those values for the AC and DC components of the voltage impressed on the rods for which a stable trajectory is obtained. FIG. 4 shows the stability diagrams obtained for a number of rod diameters. The parameters α and δ used in the figure are analogous to the a and q of the hyperbolic analyzer of FIG. 1. They are defined as

$$\alpha=\frac{e^U}{m\omega^2 r_0^2}, \qquad \delta=\frac{e^V}{m\omega^2 r_0^2}$$

The important thing to note in FIG. 4 is that these stability diagrams have the same shape but differ in size from the a–q diagrams of FIG. 2. FIG. 5 shows that if each diagram is normalized to a peak value of $\alpha=\delta=1$, all the diagrams fall on top of each other including the diagram for the hyperbolic analyzer. Thus it can be concluded that

$$\alpha=K_1 a$$

$$\text{and } \delta=K_2 q$$

and from the definitions of α, δ, a, and q it can also be seen that

$$2K_1=K_2$$

so that

$$\alpha=Ka$$

$$\delta=2Kq$$

where $K=0.125$ for the hyperbolic analyzer, FIG. 6 shows K as a function of rod radius for round rod analyzers.

It is thus apparent that a mass analyzer can be produced with rods of radius differing from the formerly prescribed 1.15 r_o where $K=0.126$.

Flat Plate Analyzer

The flat plate analyzer corresponds to the case where the rod radius becomes infinite and the analyzer takes the form shown in FIG. 7 where the plates are indicated at 22–28. The solution to Laplace's equation can be explicitly expressed for this configuration. That is,

$$\phi=\frac{4}{\pi}(U+V\cos\omega t)\sum_{\text{odd } n}\frac{1}{n}\left\{\left(\cosh\frac{n\pi}{2r_0}x\sin\frac{n\pi}{2r_0}y-\cosh\frac{n\pi}{2r_0}y\sin\frac{n\pi}{2r_0}x\right)+\left(\frac{1-\cosh n\pi}{\sinh n\pi}\right)\left(\sinh\frac{n\pi}{2r_0}x\sin\frac{n\pi}{2r_0}y-\sinh\frac{n\pi}{2r_0}y\sin\frac{n\pi}{2r_0}x\right)\right\}$$

For this potential, the equations of motion are

$$\ddot{x}=-\frac{e}{m}\frac{\partial\phi}{\partial x}, \qquad \ddot{y}=-\frac{e}{m}\frac{\partial\phi}{\partial y}$$

where x'' and y'' are the x and y components of the acceleration on the particle as a function of position and time. These are not readily integrable to give x and y as functions of time, however, they were numerically integrated using a computer to give values of α and δ, as defined before, for which an ion would have a stable trajectory. When this is done, the diagram of FIG. 8 results. Again, this normalizes onto the same diagram shown in FIG. 5 which again implies that

$$\alpha=Ka$$

$$\text{and } \delta=2Kq$$

The value for K for the square analyzer is 0.116.

Circular Concave Analyzer

If the plates of FIG. 7 are bent into segments of a circle, the electrode structure of FIG. 9 where the plates are shown at 30–36, is obtained. The potential for this case also can be written explicitly and is found to be

$$\phi=\frac{4}{\pi}(U+V\cos\omega t)\sum_{n=0}^{\infty}\frac{r^{2n+1}}{r_0^{2n+1}}\sin[2(2n+1)\theta]$$

The differential equations of motion can again be numerically integrated to give the stability diagram of FIG. 10. This figure also normalizes onto the diagram of FIG. 5 and so again

$$\alpha=Ka$$

$$\text{and } \delta=2Kq$$

The value of K for the concave analyzer is found to be 0.109. The authors (1) T. Hayashi and N. Sakudo and (2) M. Y. Bernard discussed the possibility of using circular concave electrodes. These authors, however, have approached the problem from the point of view that the hyperbolic analyzer represents the ideal and the attempt is made to select an angle subtended by the circular electrodes such that spatial components of the field higher than the quadrupole component are eliminated or, at least, minimized. The analysis presented in this disclosure point to the conclusion that such minimization is neither necessary nor even desirable. If all higher spatial field components were eliminated, leaving only the quadrupole component, the value of K would increase to 0.125, i.e., the value of K for the hyperbolic analyzer, and the advantages of the lower K value would be forfeited.

Conclusions

The invention derives from conclusions to be drawn from the foregoing analyses.

The first conclusion is that any symmetric array of four electrodes can be used for mass separation. Secondly, each array of electrodes has a particular value of K relating the α and δ parameters to the hyperbolic a and q parameters. Further implications of the second conclusion are as follows. If the following values are substituted into the expressions for the hyperbolic a and q parameters—that is $e=1.6\times10^{-19}$ coulombs, one atomic mass unit $=1.67\times10^{-27}$ kilograms, and the angular frequency $=2\pi\times10^6 f$ where f is expressed in megahertz, the following expressions are obtained.

$$a=0.194\frac{U}{Mf^2r_0^2}$$

and

$$q=0.0968\frac{V}{Mf^2r_0^2}$$

where M is the mass of the ion in atomic mass units and r_o is expressed in centimeters. The choice of resolution fixes the ratio of a and q and thus we may use the quantity $V/Mf^2r_o^2$ as a "figure of merit" for various types of electrode configuration. The lower the value of this quantity, the lower is the voltage necessary to apply to the analyzer electrodes to allow a given mass to pass through the analyzer for some given frequency and field radius. The generation of high voltages at high frequency is not a desirable condition. The operating point for high resolution for a hyperbolic analyzer is at $q=0.7068$, thus

$$\frac{V}{Mf^2r_0^2}=7.218 \text{ (hyperbolic analyzer)}$$

This parameter for several differing structures is given in the following table.

Structure	$V/Mf^2r_o^2$
hyperbolic array	7.218
1.15 r_o radius round rod	7.317
0.01 r_o radius round rod	31.8
0.001 r_o radius round rod	51.1
flat plate array	6.750
circular concave array	6.320
10 r_o radius round rod	6.918

Thus a more efficient mass analyzer is obtained in the sense that the flat plate or concave array can operate at potentials lower than the hyperbolic array given the same mass, frequency of the AC voltage, and field radius. It must be reiterated here that the results obtained for the square and concave analyzers are novel and unexpected. The computer analysis shows that specific mass separation can be achieved at lower values of K (and hence lower values of $V/Mf^2r_0^2$) than for a pure quadrupole field, i.e., the field produced by hyperbolic electrodes. Specific mass is defined to be the mass to charge ratio for an ion. The advantages are manifold: simpler electronics, higher transmission coefficient for the analyzer, lower cost construction, to name just a few. Precision ground rods are very expensive but low cost, thin, metallic ribbons (see ribbons **40–46** of FIG. **12**) can be stretched to give a very precise flat surface for a flat plate array or precision bore quartz tubing (see **50** of FIG. **13**) can be obtained at very modest cost with the inside metallized (see **52–56** showing three of the electrodes in FIG. **13**) to produce a concave array. The small wire (see wires **60–66** of FIG. **14**) analyzers (0.01 r_o and 0.001 r_o rod sizes, for example) do not have the advantage of low voltages but they allow very open light construction with the "rods" consisting of taut wires. For a small mass range application such as upper atmosphere research, such a structure has the advantage of very low weight. It is clear from the analysis presented in this disclosure that many other electrode forms may be used to advantage in differing applications. Thus, the teaching that the hyperbolic electrode analyzer is the optimum electrode structure and that a round rod structure with rod radius equal to 1.15 r_o is the best approximation to the hyperbolic structure is not true for all applications. Structures with K values differing from these two have many superior characteristics. The analysis presented in this disclosure has been presented in terms of electrostatic fields for the purpose of specific mass analysis in a "quadrupole" type structure. However, the analyses are equally valid for pole face contour in magnetic quadrupoles. These magnetic quadrupole structures are used in the analysis by specific mass of high energy particles as found in nuclear accelerators.

Referring to FIG. **11**, there is shown a nonsymmetric quadrupole structure having upper and lower plates **90** and **92** which extend over the plates **94** and **96** to thereby provide a stable mechanical structure. Although, as stated above the quadrupole is nonsymmetric it is nevertheless illustrative of an instance of a structure wherein the value of K is different from 0.125 but nevertheless useful in some applications.

The quadrupole-type analyzers described hereinbefore are satisfactory in resolution performance, but because of the presence of relatively large amplitude, nonquadrupole field components, the effective usable cross section of the analyzer is restricted for some applications. For example, the usable radius of the concave analyzer of FIG. **9** is 60 percent of r_o where r_o is the radius of the electrodes. Thus the available cross section usable as an analyzer in the concave device is only 36 percent of the geometric cross section of the analyzer structure. The result of this is to reduce the sensitivity of the device.

Referring to FIG. **15**, there is shown an electrode structure comprising electrodes **70–76** together with enclosing cylinder **78** which typically is grounded as indicated at **79**. It can be shown from the solution of Laplace's equation in cylindrical coordinates that the potential within the electrodes **70–76** can be expressed in the form

$$\phi(r,\theta)=C_0\left(\frac{r}{r_o}\right)^2\cos 2\theta+C_1\left(\frac{r}{r_0}\right)^6\cos 6\theta$$

$$+C_2\left(\frac{r}{r_0}\right)^{10}\cos 10\theta+\ldots+C_n\left(\frac{r}{r_0}\right)^{2(2n+1)}\cos 2(2n+1)\theta+\ldots$$

where r is the distance from the center of the electrode structure.

The values obtained for the coefficients C_0, C_1, C_2, ... are determined by the specific electrode structure chosen. For the concave analyzer,

$$C_n=\frac{8V_0}{\pi}\left\{\int_0^{\gamma}\cos 2(2n+1)\theta d\theta+\int_{\gamma}^{\pi/4}\phi(\theta)\cos 2(2n+1)\theta d\theta\right\}$$

where γ is one half the angle subtended by an electrode and $\phi(\theta)$ is the potential along the circular extension of the electrode in the gap between adjacent electrodes as indicated at **77** in FIG. **15**.

Referring to FIG. **16**, there is shown a square analyzer comprising electrodes **80–86** and enclosing cylinder **88** which typically is grounded as indicated at **89**. For the square analyzer, the coefficients are somewhat more complex

$$C_n=\frac{V_0}{2^{4n}(2(2n+1))!}\left(\frac{\pi}{2}\right)^{2(2n+1)}\sum_{k=1}^{\infty}\frac{(2k-1)^{2(2n+1)}}{\cosh\left[\frac{(2k-1)\pi}{2r_0}\right]}$$

$$\left\{\int_0^{l}\cos\frac{(2k-1)\pi}{2r_0}ydy+\int_{l}^{r_0}\phi(r_0,y)\cos\frac{(2k-1)\pi}{2r_0}ydy\right\}$$

Here $\phi(r_o, y)$ is the potential along the extension of any one of the electrodes **80–86** to its corresponding corner of the square as indicated for electrodes **84** and **82** at **85** and **87** for example. l is the half width of the electrode.

The first term in the expansion of the potential for either of the structures of FIGS. **15** and **16** is the quadrupole term. The second is a 12-pole term, the third is a 20-pole term, etc. Since the C_1 term is the second largest term in the expansion (C_2 is considerably less than C_1), one can most closely approximate the hyperbolic potential distribution by adjusting the electrode size such that C_1=0. It has been determined that C_1 is approximately 10 percent of C_0 for the square analyzer of FIG. **7**. Thus, a deviation of 10 percent would be acceptable with the square analyzer but preferably C_1 should be made as small as possible. Further, in fact, the value of C_1 can be greater than 10 percent of C_0 in some configurations such as the concave analyzer of FIG. **9** where C_1 is 33 percent of C_0.

The potential in the gaps between the electrodes depends on the potential distribution surrounding the electrode structure. A mass analyzer is normally operated within a vacuum system of finite size and therefore surfaces, either grounded or operating at some other potential, occur in the vicinity of the electrode structure of the mass analyzer. These surfaces influence the potential distribution in the vicinity of the electrode structure and therefore influence the values of the coefficients, C_n. It therefore follows that the size of each electrode, for which C_1=0, is influenced by the presence of the external surfaces.

A computer was used to determine the potential in the gaps between electrodes for the concave and square analyzers located inside a grounded cylinder such as cylinders **78** and **88** of FIGS. **15** and **16** respectively. A grounded cylinder was chosen to illustrate the effect of external surfaces because it represents the condition most often encountered in actual practice. That is, a mass analyzer operating in a vacuum system most often is surrounded by a vacuum tight housing consisting of a metal tube which is electrically grounded. This housing is open on one end so that it may be attached to the remainder of the vacuum chamber in which the materials to be analyzed are generated. It should be understood, however, that this case is illustrative only and the technique used here may be applied to any arrangement of surfaces with any chosen potentials.

The Liebmann numerical process was used to solve Laplace's equation for a series of grounded surface radii and the potential in the gaps between electrodes was obtained. The integral in the expression for C_1 was then numerically evaluated and thus C_1 was obtained as a function of the electrode size. The electrode size which gave C_1=0 was then obtained. If, as in FIG. **15**, R is the radius of the grounded surface, and r_o is the geometric radius of the analyzer, then the angle, 2γ, subtended by the electrode in the concave analyzer for C_1=0 is given by

$$2\gamma = 44.02 - 2.941\left(\frac{r_0}{R}\right) + 5.592\left(\frac{r_0^2}{R}\right) + 8.848\left(\frac{r_0^3}{R}\right) \text{deg.}$$

Similarly, as in FIG. 2, the width of the electrode, $2l$, in the square analyzer for $C_1=0$ is given by

$$\frac{2l}{r_0} = 0.8824 + 0.1512\left(\frac{r_0}{R}\right) - 0.0924\left(\frac{r_0}{R}\right)^2 + 0.0670\left(\frac{r_0}{R}\right)^3$$

Here r_o is the distance from the center of the electrode structure to the electrode surface and the calculated length is given as a fraction of r_o to give a dimensionless quantity.

If a representative example is taken and a stability diagram obtained, then it is observed that the peak shifts toward the α and δ values of the hyperbolic analyzer as C_1 approaches zero.

The K value for the concave analyzer shifts from a value of 0.109 for 90° electrodes to 0.118 for the case where $C_1=0$. The K value for the square analyzer shifts from 0.116 for $l=r_o$ to 0.123 for the case where $C_1=0$. The K value of a hyperbolic analyzer is 0.125. Thus it is apparent that the optimization of the electrode size has brought the field closer to that of a pure quadrupole. For the square analyzer, the effective radius usable for mass analysis increases from 0.6 r_o to 0.85 r_o as K increases from 0.116 to 0.123. Since the available area, and thus the sensitivity of the instrument, increases as the square of the radius, the sensitivity increases by almost 100 percent as K increases from 0.116 to 0.123. Similarly for the concave analyzer, as K increases from 0.109 to 0.118, the effective radius increases from 0.6 r_o to 0.75 r_o or an increase in sensitivity by almost 60 percent.

Numerous modifications of the invention will become apparent to one of ordinary skill in the art upon reading the foregoing disclosure. During such a reading it will be evident that this invention provides a unique quadrupole device for accomplishing the objects and advantages herein stated.

What is claimed is:

1. A quadrupole mass analyzing device for analyzing charged particles by charge to mass ratio comprising four flat plate electrodes disposed within the device where a first nonadjacent pair of said electrodes is separated by a first distance and a second nonadjacent pair of said electrodes is separated by a second distance, and means for applying superimposed DC and sine wave AC voltages to said electrodes, the voltages applied to said first pair of electrodes being equal and the voltages applied to said second pair of electrodes being equal and being opposite in polarity to the voltages applied to the first pair of electrodes.

2. A quadrupole device as in claim 1 where said first distance equals said second distance.

3. A quadrupole device as in claim 2 where said first pair of electrodes are parallel to one another and said second pair of electrodes are parallel to one another.

4. A quadrupole device as in claim 1 where said first pair of electrodes are parallel to one another.

5. A quadrupole device as in claim 4 where said second pair of electrodes are parallel to one another.

6. A quadrupole device as in claim 4 where said second pair of electrodes are coplanar.

7. A quadrupole device as in claim 6 where each of said second pair of electrodes is (1) narrower in width than each of said first pair of electrodes and (2) disposed between said first pair of electrodes.

8. A quadrupole mass analyzing device for analyzing charged particles by charge to mass ratio comprising four flat plate electrodes symmetrically disposed within the device where a first nonadjacent pair of said electrodes has applied thereto a first voltage ($U+V\cos wt$) and a second nonadjacent pair of said electrodes has applied a second voltage $-(U+V\cos wt)$ thereto where

U=a DC voltage;
V=the half-amplitude of an AC voltage;
w=the angular frequency of the AC voltage; and
t=time.

9. A quadrupole device as in claim 8 where each said flat plate is disposed in proximity to the two plates adjacent to it so that the array of said plates is square in cross section.

10. A quadrupole device as in claim 8 where said plates are disposed parallel with respect to one another.

11. A quadrupole device as in claim 8 where each of said flat plates comprises a thin, metallic ribbon disposed on a support.

12. A quadrupole device as in claim 8 where said device includes at least one source of potential in addition to the DC and AC voltages applied to said four electrodes, the dimensions of each electrode being such that the coefficient C_1 in the expression $\phi(r,\theta)=C_0(r/r_0)^2\cos 2\theta+C_1(r/r_0)^6\cos 6\theta+\cdots C_n(r/r_0)_+^{1}\cos 2(2n+1)\theta$
where $\phi(r,\theta)$=the potential due to the applied fields at radius r and angle θ with respect to the axis of symmetry of said electrodes, r_o=the distance from the axis of symmetry to said electrodes, and C_1, $C_2\cdots C_n$ are constants defined by the potentials applied and the dimensions of the structure, is no more than 10 percent of the value of C_0.

13. A quadrupole device as in claim 12 where the potential is the potential on a cylindrical tube which surrounds said four electrodes and where each said flat plate is disposed in proximity to the two plates adjacent to it so that the array of said plates is square in cross section.

14. A quadrupole device as in claim 13 where said cylindrical tube is grounded.

15. A quadrupole device as in claim 14 where said plates are symmetrically disposed within said tube, the radius of said tube being R and where the width, $2l$, of each plate is approximately specified as follows:

$$\frac{2l}{r_0} = 0.8824 + 0.1512\left(\frac{r_0}{R}\right) - 0.0924\left(\frac{r_0}{R}\right)^2 + 0.0670\left(\frac{r_0}{R}\right)^3$$

where r_o=the distance from the center of said array of plates to the surface to said plates.

* * * * *